King Saud University

Arabian Journal of Chemistry

www.ksu.edu.sa
www.sciencedirect.com

ORIGINAL ARTICLE

cis-bis(N-benzoyl-N′,N′-dibenzylthioureido) platinum(II): Synthesis, molecular structure and its interaction with human and bovine serum albumin

CrossMark

Rodrigo S. Correa [a],[*], Katia M. Oliveira [b], Hiram Pérez [c], Ana M. Plutín [d], Raúl Ramos [d], Raúl Mocelo [d], Eduardo E. Castellano [e], Alzir A. Batista [b]

[a] *Departamento de Química, ICEB, Universidade Federal de Ouro Preto, CEP 35400-000 Ouro Preto, MG, Brazil*
[b] *Departamento de Química, Universidade Federal de São Carlos, São Carlos, São Paulo, Brazil*
[c] *Departamento de Química Inorgánica, Facultad de Química, Universidad de la Habana, Habana 10400, Cuba*
[d] *Laboratorio de Síntesis Orgánica, Facultad de Química, Universidad de la Habana, Habana 10400, Cuba*
[e] *Instituto de Física de São Carlos, Universidade de São Paulo, São Carlos, SP, Brazil*

Abstract In this paper, the title compound was synthesized from N-benzoyl-N′,N′-dibenzyl thiourea ligand and potassium tetrachloroplatinate(II), and its interaction with human (HSA) and bovine (BSA) serum albumin was evaluated. Also, the crystal structure was determined from single-crystal X-ray diffraction, confirming that the platinum atom is coordinated with two chelated N-benzoyl-N′,N′-dibenzylthiourea ligands in a distorted square-planar geometry. In the solid state, Hirshfeld surface analysis emphasizes that the molecules are connected by non-classical C–H⋯C, C–H⋯S and H⋯H intermolecular contacts. These weak interactions can be mainly responsible due to complex-BSA and complex-HSA binding. The complex interacts differently with HSA and BSA such as observed by the binding constant, K_b, presenting values of around $10^5 \, M^{-1}$ and $10^4 \, M^{-1}$, respectively. Thermodynamic parameters (ΔG, ΔH and ΔS) suggest spontaneous interactions between complex and the proteins.

* Corresponding author. Tel.: +55 1633518285; fax: +55 1633518350.
E-mail address: rodrigocorrea@iceb.ufop.br (R.S. Correa).
Peer review under responsibility of King Saud University.

ELSEVIER **Production and hosting by Elsevier**

1. Introduction

N-acylthioureas have attracted increasing attention in the last two decades as bioactive agents and ligands that can coordinate to metal species (Aly et al., 2007; Saeed et al., 2013; Saeed et al., 2014a,b). A rapid survey of the literature shows that a number of papers on crystal structures has been

published concerning the coordination ability of benzoylthioureas with transition metal ions, and particularly with regard to coordination behavior toward platinum(II) ion (Bourne and Koch, 1993; Koch and Bourne, 1998; Westra et al., 2004, 2005). Special interest has been given to the acquisition of complexes that are not structurally analogous to cisplatin [Pt(NH$_3$)$_2$Cl$_2$] to overcome its major drawbacks, studies are extended toward new platinum(II)-based antitumor drugs, focused on the use of the oxygen–sulfur acylthiourea chelate ligand systems (Sacht et al., 2000a,b). More recently, there have been efforts directed at the design of non-classical Pt complexes. These include the investigation of interactions of a series of antitumor platinum acylthiourea complexes with natural and synthetic DNA and with nucleotides (Rodger et al., 2002), as well as antitumor and antifungal biological activity and inhibitory activities against viruses (Mihai and Negoiu, 2012). Moreover, luminescence properties of a series of Pt(II) complexes bearing N-benzoylthiourea derivatives have been investigated, which find applications in optoelectronic devices, luminescent probes for biomolecules and chemical sensors (Cîrcu et al., 2009).

In the past few years, our research group has been interested in the synthesis (Pérez et al., 2011a,b,c; O'Reilly et al., 2012), characterization, crystal structure (Pérez et al., 2011a, b,c, 2012a,b), and antifungal (O'Reilly et al., 2012) and antitumor (Plutín et al., 2014; Correa et al., 2015) activities of some disubstituted acylthiourea derivatives and their metal complexes. Therefore, as part of our ongoing studies, we report here the synthesis, characterization and molecular structure of cis-bis(N-benzoyl-N′,N′-dibenzylthioureido)platinum(II) complex, as well as a detailed study of it intermolecular contacts based on the Hirshfeld surface. Furthermore, its interactions with the HSA and BSA macromolecules were evaluated.

2. Experimental

2.1. Instrumentation

The determination of C/H/N/S was done using a Fisons – EA-1108 CHNS Element Analyzer. The IR spectrum was recorded on a FT-IR Bomem-Michelson 102 spectrometer in the 4000–200 cm^{-1} region using KBr pellets. ^{1}H and ^{13}C NMR spectra were recorded on a Bruker DRX 400 MHz using CDCl$_3$ as the solvent, internally referenced to TMS. Single crystal X-ray diffraction data were collected on an Enraf–Nonius Kappa-CCD diffractometer for the title compound, using monochromated Mo Kα radiation. The structure was solved (Sheldrick, 2008) by direct and conventional Fourier methods with full-matrix least-squares refinement (Sheldrick, 2008) based on F^2. All non-hydrogen atoms were refined anisotropically; geometrically placed hydrogen atoms were refined with a 'riding model' and U(H) = 1.2 U(C$_{iso}$) and 1.5 U(C$_{iso}$) for aromatic and methylene groups, respectively. Software used to prepare material for publication: WinGX (Farrugia, 2012), ORTEP-3 for Windows (Farrugia, 1997) and Mercury (Macrae et al., 2006). Further details concern data collection and refinement.

2.2. Synthesis of cis-bis(N-benzoyl-N′,N′-dibenzylthioureido) platinum(II) complex

The N-benzoyl-N′,N′-dibenzylthiourea ligand was prepared using the standard procedure previously reported by Nagasawa and Mitsunobu, 1981 for the reaction of benzoyl chloride with KSCN in anhydrous acetone, and then condensation with dibenzylamine. To a methanol solution (30 ml) containing the ligand (1.29 g, 2 mmol), a methanol solution of K$_2$[PtCl$_4$] (0.42 g, 1 mmol) was added. The solution was stirred at room temperature for 2 h. The mixture was filtered and the filtrate was evaporated under reduced pressure producing a yellow solid, which was washed with water and hexane. Single crystals were obtained by slow evaporation of a methanol/N-hexane/ethyl ether solution (3:1:1, v/v/v) of the complex.

cis-bis(N-benzoyl-N′,N′-dibenzylthioureido)platinum(II): Yellow. Yield: 83%. M.p.: 164–165 °C. Anal. calcd. For C$_{44}$H$_{38}$N$_4$O$_2$S$_2$Pt: C, 57.82; H, 4.19; N, 6.13; S, 7.02. Found: C, 57.96; H, 4.30; N, 6.26; S, 6.87%. Molar conductance (μS/cm, CH$_2$Cl$_2$) 2.1. FT-IR (KBr, cm^{-1}): 2972, 2921(CH), 2860 (CH$_2$), 1551 (C–C) (phenyl), 1500 (C–N), 1498 (C–O). ^{1}H NMR (400 MHz, CDCl$_3$, δ, ppm): 8.28–8.26 (m, 2H, Ar–H), 7.52–7.24 (m, 13H, Ar–H), 5.09 (s, 2H, –CH$_2$), 4.94 (s, 2H,–CH$_2$). ^{13}C NMR (150 MHz, CDCl$_3$, δ, ppm): 170.28 (C–S), 169.65 (C–O), 167.39 (1C, Ar–C), 136.30 (1C, Ar–C), 135.17–127.33 (16C, Ar–C), 53.94 (1C, –CH$_2$), 51.78 (1C, –CH$_2$).

2.3. Human serum albumin (HSA) and Bovine serum albumin (BSA) interaction studies

The HSA and BSA binding experiment of the complex was performed by tryptophan fluorescence quenching in Tris–HCl buffer (pH = 7.4). The quenching experiments were performed using the platinum complex in different molar ratios in an opaque 96 well plate, using the fluorimeter Synergy/H1-Biotek. The fluorescence spectra were recorded at 298 and 310 K temperature with an excitation wavelength at 270 nm for BSA and HSA, and emission wavelength at 320 nm for BSA and 305 nm for HSA. The concentration of BSA (2.5 μM) and HSA (5 μM) was kept constant while varying the complex concentration from 0 to 25 μM in Tris–HCl buffer (pH = 7.4) containing 5% DMSO.

3. Results and discussion

3.1. Complex characterization and molecular structure

The analytical and spectroscopic data of the title complex are in agreement with the structure containing two benzoylthiourea per platinum, with the ligand coordinated to metal center as monoanionic in order to form a neutral complex as suggested by molar conductance. The main vibrational bands are given in the experimental section. Some important conclusions can be made, mainly those in the high-frequency region, where the free N-benzoyl-N′,N′-dibenzylthiourea presents the νN–H stretching band at 3200 cm^{-1}; meanwhile, this band is not present in the spectrum of the Pt(II) complex. This suggests that the ligand is deprotonated after coordination. Also, ^{1}H NMR spectrum of the free ligand presents a shoulder band due to a singlet of the N–H proton at about 9.0 ppm. However, this kind of signal is absent in the spectrum of the complex, suggesting the deprotonation of the acylthioureide group by the coordination of the ligand with Pt(II).

The crystal structure of complex determined by single-crystal X-ray diffraction confirms the proposed structure. It

Table 1 Crystal data and structure refinement for the title compound.

Empirical formula	$C_{44}H_{38}PtN_4O_2S_2$
Formula weight	913.99
Temperature (K)	296(2)
Crystal system	Orthorhombic
Space group	$P2_12_12_1$
a, b, c (Å)	5.5579(1), 19.7893(3), 34.1642(6)
Volume (Å³)	3757.7(1)
Z	4
ρcalc. (mg mm⁻³)	1.616
μ (mm⁻¹)	3.889
$F(000)$	1824
Crystal size (mm³)	0.26 × 0.04 × 0.04
2θ range for data collection	2.66–25.98°
Index ranges	$-6 \leqslant h \leqslant 6, -24 \leqslant k \leqslant 24,$ $-42 \leqslant l \leqslant 42$
Reflections collected	37,340
Independent reflections	7328 [R(int) = 0.083]
Data/restraints/parameters	7328/0/478
Goodness-of-fit on F^2	0.997
Final R indexes [$I > 2\sigma (I)$]	R1 = 0.0344, wR2 = 0.0777
Final R indexes [all data]	R1 = 0.0452, wR2 = 0.0827
Largest diff. peak/hole (e Å⁻³)	0.951 and −1.002
Absolute structure parameter	0.030(6)

crystallizes in the orthorhombic space group, $P2_12_12_1$ with unit cell dimensions of a = 5.5579 (1) Å, b = 19.7898 (3) Å, c = 34.1642 (6) Å, and V = 3757.7 (1) Å³ (Table 1). The metal is bischelated by two N-benzoyl-N′,N′-dibenzylthiourea molecules adopting a *cis* configuration. As can be seen in Fig. 1, the ligand is coordinated to the central ion by two S and two O atoms. Selected bond lengths and angles are listed in Table 2. The coordination geometry of complex is a slightly distorted square-plane as reflected by O2–Pt–S1 and O1–Pt–S2 angles of 178.1(1)° and 177.3(1)°, respectively. The Pt–O bond distances [2.074(4) and 2.026(4) Å] are very similar to related structures (Hernández et al., 2003a,b). As expected, Pt–O bond distances are shorter than Pt–S bond distances [2.226(2) and 2.229(2) Å].

The bond lengths of carbonyl and thiocarbonyl groups, as well as the C–N bond distances are in agreement with those found in similar compounds (Binzet et al., 2012a,b; Arslan et al., 2006). Compared to the structure reported for the free ligand (Gunasekaran et al., 2010), the C–O [1.266(7) Å] and C–S [1.730(6) Å] average bond distances for the title complex are longer than the averaged values found for the two independent molecules in the ligand (C–O 1.218(4) and C–S 1.677(3) Å). In addition, the (O)C–N [1.324(7) Å] and (S)C–N [1.340(7) Å] average bond lengths in the complex are shorter than the related in the ligand [1.384(4) and 1.403(4) Å]. These results can be explained by the existence of electron delocalization within the chelate rings.

The largest distances of platinum, sulfur, and oxygen atoms from the best plane through the coordination sphere are −0.0012(1), −0.0202(1), and 0.0232(1) Å, respectively. The chelate rings, Pt–O1–C12–N12–C11–S1 and Pt–O2–C22–N22–C21–S2, are nearly planar, and the largest deviations from the best plane are 0.1561(1) Å for S2 and −0.1275(1) Å for Pt.

On the other hand, the value of dihedral angle between the chelate planes for the title complex is 13.1(2)°, being notably higher than for homologous complexes with diphenyl [average 3.6(1)°] (Hernández et al., 2003a,b) and diethyl [1.6(1)°] (Sacht et al., 2000a,b) substituents. In addition, the same trend was found in the corresponding nickel complexes, the dihedral angle between the chelate rings increasing in the order diethyl, 3.3 (1)° (Knuuttila et al., 1980) < diphenyl, 6.7(1)° (Pérez et al., 2012a,b) < dibenzyl, 13.3(2)° (Pérez et al., 2008). These results indicate the role of substituents in the benzoylthiourea moiety on the molecular conformation of these complexes.

The two benzyl groups attached to N11 atom are inclined toward each other at an angle of 22.0(2)°, and their aromatic rings are linked by an intramolecular edge-to-face π–π interaction (Hunter, 1994). The Cg1 (ring C112–C117) and Cg2 (ring C122–C127) centroids are separated by a distance of 4.144(2) Å, and slip angles (the angle between the centroid vector and the normal to the ring plane) of 14.8 and 17.8°, and θ angle
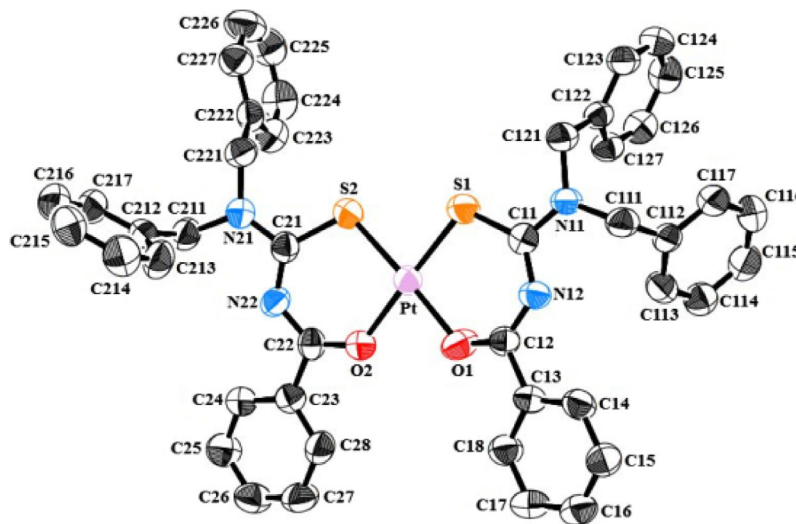

Figure 1 *ORTEP* view of the title compound, with atom-numbering. Hydrogen atoms are omitted for clarity. Displacement ellipsoids are drawn at the 50% probability.

Table 2 Bond lengths (Å) and angle lengths (°) for the Pt(II) complex.

Bond lengths						Angle lengths	
Pt–O1	2.017(4)	O1–C12	1.272(7)	N22–C21	1.334(7)	O1–Pt–O2	83.14(16)
Pt–O2	2.026(4)	O2–C22	1.259(7)	N22–C22	1.324(7)	O1–Pt–S1	95.47(13)
Pt–S1	2.226(2)	N12–C11	1.345(7)	N21–C21	1.343(7)	O2–Pt–S1	178.13(12)
Pt–S2	2.229(2)	N12–C12	1.324(7)	N21–C211	1.450(7)	O1–Pt–S2	177.32(14)
S1–C11	1.720(6)	N11–C11	1.354(7)	N21–C221	1.468(7)	O2–Pt–S2	94.42(12)
S2–C21	1.740(6)	N11–C111	1.480(7)	N22–C21	1.334(7)	S1–Pt–S2	86.99(6)

Table 3 Hydrogen-bonding geometry for the title compound (Å, °).

D–H···A	d(D–H)	d(H···A)	d(D–A)	∠(D–H···A)
C16–H16···C113[i]	0.93	2.88	3.623(9)	137
C123–H123···C123[ii]	0.93	2.87	3.743(9)	158
C124–H124···S1[ii]	0.93	3.16	3.966(6)	146
C125–H125···S2[ii]	0.93	3.26	4.047(6)	145

Symmetry codes: (i) $-\frac{1}{2} + x$, $\frac{1}{2} - y$, $1 - z$; (ii) $\frac{1}{2} + x$, $3/2 - y$, $1 - z$.
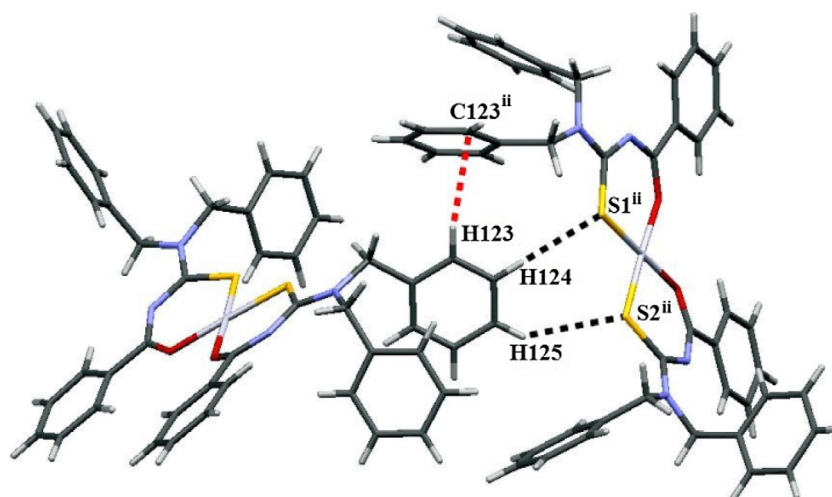
Figure 2 View of molecules linked by C–H···C (red) and C–H···S (black) hydrogen bonding (dashed lines) [symmetry code: (ii) $\frac{1}{2} + x$, $1.5 - y$, $1 - z$].

(Cg2-C113-Cg1 angle) of 58.1° for the title complex are normal (valid) aromatic stacking values (Correa et al., 2012). This π–π interaction is not observed between the benzyl groups linked to N21 atom, being 48.3°, the value of related dihedral angle.

We observed a similar type of stacking occurring in the isostructural homologous Ni(II) complex, previously reported for our group (Pérez et al., 2011a,b,c), where the angles between the corresponding benzyl groups, inter-centroid distance, and slip angles values are 21.2(2)°, 4.127(2) Å, 14.6°, 18.4°, respectively. The θ angle value for Pt(II) complex is lower than for the Ni(II) complex (88.6°), and both these values are within the expected range (Hunter, 1994). It is interesting to observe that intramolecular π–π interaction is not found in the free ligand (Gunasekaran et al., 2010). These results indicate that this type of interaction is present in the title complex as a clear effect of crystal forces on the molecular conformation.

Aromaticity of the acylthiourea moiety in each ligand of the complex was measured based on Harmonic Oscillator Model of Aromaticity (HOMA) index. It is assumed that HOMA values close to 0 occur for non-aromatic systems, and values equal to 1 occur for systems with π-electrons that are fully delocalized (Frizzo and Martins, 2012). The S1–C11–N12–C12–O1 and S2–C21–N22–C22–O2 acylthiourea moieties present the calculated HOMA index of 0.9486 and 0.8917, respectively, and suggest that both acylthiourea moieties in the complex are more resonant than the free ligand with HOMA value of 0.7572.

The molecules in the crystal are linked by weak nonclassical C–H···C and C–H···S hydrogen-bonding interactions. In addition, short repulsive H···H intermolecular contacts are formed between two aromatic C–H groups, in such a way that the H atoms approach quite closely with an average distance of 2.302(2) Å and an average bond angle of

139°, being the stronger interaction contributing to crystal stabilization (Table 3 and Fig. 2).

The intermolecular interactions of the title complex were analyzed using the Hirshfeld surfaces and the corresponding 2D fingerprint plots (Spackman and Jayatilaka, 2009; Spackman and McKinnon, 2002). Hirshfeld surface analyses were carried out and fingerprint plots were plotted using CrystalExplorer 3.0 (Wolff et al., 2009). For points on the surface, d_e and d_i are defined as the distance from the surface to the nearest atom external and internal to the surface, respectively. The d_{norm} (normalized contact distance) surface and the breakdown of fingerprint plots are used for decoding and quantifying intermolecular interactions in the crystal lattice.

In the two-dimensional fingerprint diagrams, we can identify and compare the types of intermolecular interactions present in the crystal (Correa et al., 2010). Fingerprint plots for the main contacts (H···H, C···H and S···H) are shown in Fig. 3. This analysis immediately reveals that the shortest contacts correspond to the very close H···H contacts, which show a sharp spike centered near a $(d_e + d_i)$ sum of 2.1 Å [H116···H225^{iii} and H225···H116^{iv} both are 2.302(2) Å;

symmetry codes: (iii) $1.5 + x$, $1.5 - y$, $1 - z$; (iv) $1.5 + x$, $1.5 - y$, $1 - z$] (Fig. 3a). Fig. 3b isolates C···H contacts with less sharper spikes centered around $(d_e + d_i)$ of 2.8 Å, and Fig. 3c isolates S···H contacts, which show spikes centered around $(d_e + d_i)$ of 3.1 Å, corresponding to specific intermolecular C–H···C and C–H···S hydrogen bonding, respectively. These bond lengths are in agreement with those obtained in crystal structure determination (Table 3). The relative fingerprint contributions to the Hirshfeld surface area due to H···H, C···H and S···H intermolecular contacts are 57.0%, 29.4% and 4.5%, respectively.

Other smaller contributions occur for O···C (2.6%), O···H (1.2%), and O···N (0.7%) contacts. In comparison, these results are very similar to those for the homologous Ni(II) complex (Pérez et al., 2011a,b,c), which presents relative contributions of 57.9%, 29.2% and 4.4% due to H···H, C···H and S···H intermolecular contacts, respectively (re-calculated in this work). This emphasizes the importance of Hirshfeld surface and fingerprint-plot analysis for a full understanding of non-classical hydrogen-bonding and short intermolecular contacts in acylthiourea metal complex derivatives.
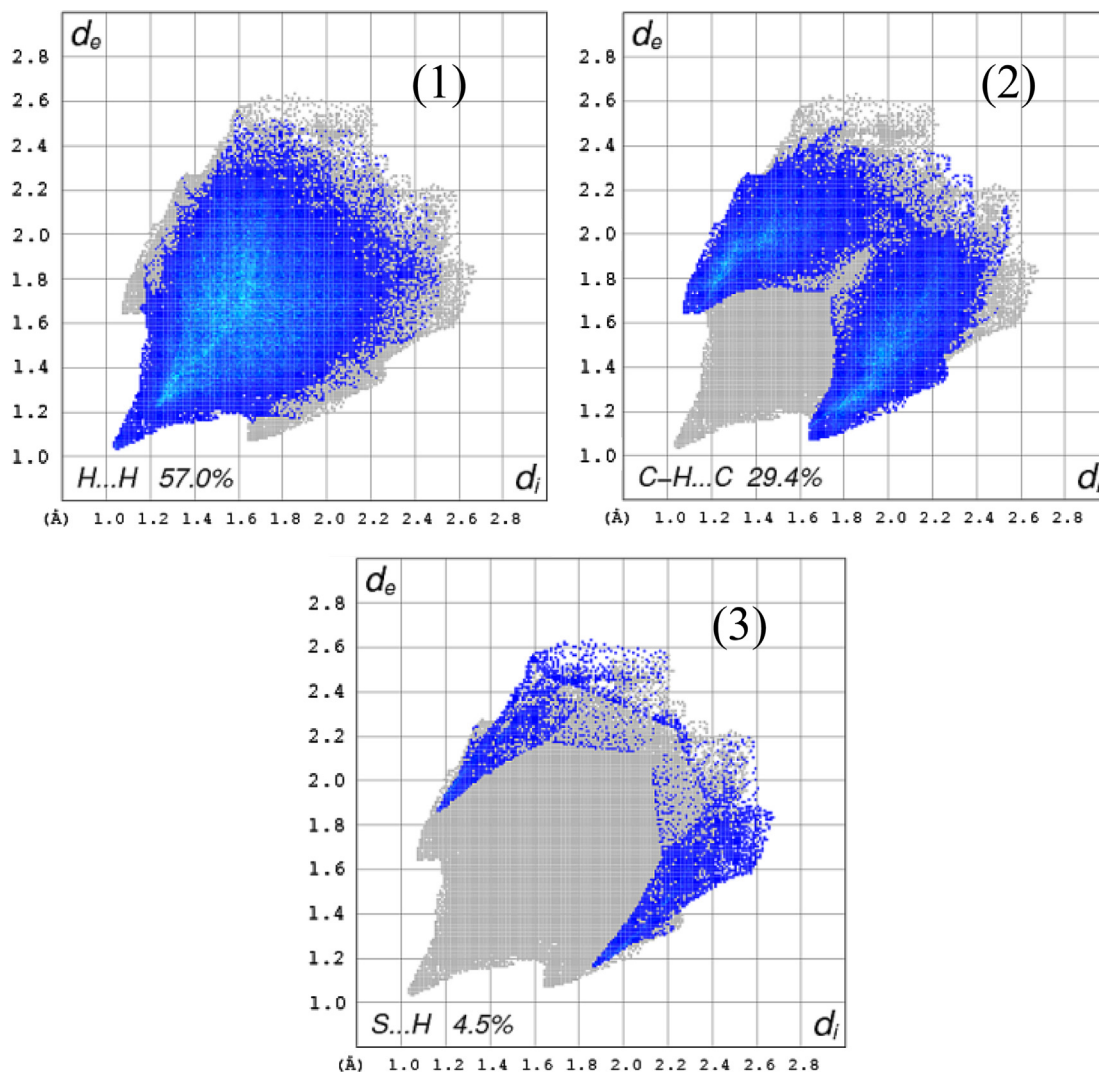

Figure 3 Fingerprints of the title compound, (a) H···H, (b) C···H, (c) S···H. The outline of the full fingerprint is shown in gray.
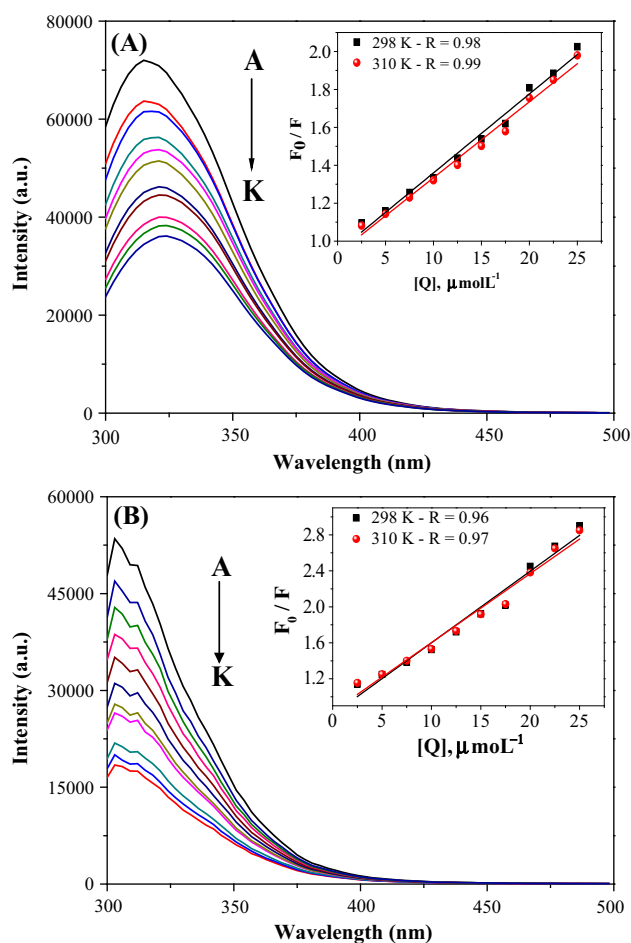
Figure 4 Fluorescence emission spectra of the BSA (2.5 μM; λ_{ex} = 270 nm) and HSA (5 μM; λ_{ex} = 270 nm) at different concentrations of complex Pt(II) at 310 K.

3.2. HSA and BSA binding studies

The interactions of the Pt complex with human serum albumin (HSA) and bovine serum albumin (BSA) were evaluated by fluorescence quenching. BSA exhibits very similar chemical structure to HSA; therefore, both albumins have been widely applied in the study of interaction with candidate of drugs. The fluorescence of HSA and BSA occurs due to tryptophan residues with a contribution of tyrosine and phenylalanine (Ganeshpandian et al., 2014). Metallodrugs candidate compounds can bind to this protein, and lead to loss or improvement of activity depending on the strength of the bond with

the protein. This is because serum albumins are the most abundant protein in plasma and are responsible for transporting drugs, metal ions, and compounds through the bloodstream (Das et al., 2015).

Therefore, the binding experiments with HSA and BSA were carried out using the platinum complex reported here, at two different temperatures (298 and 310 K), in order to evaluate the interaction between protein–Pt complex and the mechanism of interaction. Fig. 4 depicts the fluorescence emission spectra for BSA (Fig. 4a) and HSA (Fig. 4b), showing the fluorescence intensity decreasing when concentration of platinum complex is increased. The fluorescence quenching can be described by Stern–Volmer equation as follows:

$$F_0/F = 1 + K_{sv}[Q] = 1 + k_q\tau_0[Q]$$

where F_0 and F are the fluorescence intensities of HSA or BSA in the absence and presence of the platinum complex, respectively. K_{sv} is the Stern–Volmer quenching constant, k_q is the bimolecular quenching constant and τ_0 is the lifetime of the fluorescence in the absence of quencher (τ_0 = 6.2 ns) and [Q] is the concentration of a quencher (platinum complex) (Ganeshpandian et al., 2014; An et al., 2017).

The Stern–Volmer plot for the HSA and BSA fluorescence quenching by platinum complex at different temperatures is displayed in Fig. 4. All plots exhibited a good linear relationship. The values of K_{sv} and k_q at different temperatures are given in Table 4. The quenching of HSA and BSA can occur by two mechanisms: dynamic and static quenching. Dynamic quenching refers to the collisional process between the fluorophore and the quencher (in this case, platinum complex) during the transient existence of the exited state. In the static quenching occurs the formation of the fluorophore–quencher in the ground state (Ganeshpandian et al., 2014). To differentiate the dynamic and static mechanism it is necessary to evaluate the behavior at different temperatures. Dynamic quenching depends on the collisions between the fluorophore and the quencher in excited state, and these collisions increase with increasing temperature, as occurs a decrease in the viscosity of the environment. Thus, the increase in temperature leads to an increase of the constant in the case of dynamic mechanism. On the other hand, in the static mechanism the albumin-complex adduct formation decrease when temperature increase (Ganeshpandian et al., 2014).

The results represented in Table 4 show that at high temperature, high K_{sv} values are observed, which indicates the probability of a static quenching mechanism. In addition, another important aspect that indicates the presence of a static mechanism is the k_q values ($\sim 10^{12}$ M^{-1} s^{-1}) which are much higher than the maximum observed for a dynamic mechanism (2×10^{10} M^{-1} s^{-1}) (Sharma et al., 2014).

Table 4 The quenching constants (K_{sv}), (k_q), binding constants (K_b), number of binding sites (n) for the interactions of complex Pt(II) with BSA and HSA.

Albumin	T (K)	K_b (M^{-1})	$K_{sv} \times 10^4$ (M^{-1})	$k_q \times 10^{12}$ (M^{-1} s^{-1})	n
HSA	298	$(3.39 \pm 0.50) \times 10^5$	(8.11 ± 0.15)	13.08	1.16
	310	$(2.67 \pm 0.46) \times 10^5$	(7.65 ± 0.06)	12.34	1.13
BSA	298	$(4.87 \pm 0.13) \times 10^4$	(4.24 ± 0.08)	6.84	1.04
	310	$(2.61 \pm 0.81) \times 10^4$	(4.01 ± 0.01)	6.47	0.98

Table 5 The thermodynamic parameters relative of Pt(II) complex with BSA and HSA at different temperatures (298 and 310 K).

Albumin	T (K)	$\Delta H°$ (kJ mol^{-1})	$\Delta G°$ (kJ mol^{-1})	$\Delta S°$ (J mol^{-1} K^{-1})
HSA	298	−15.28	−31.55	54.59
	310		−32.20	
BSA	298	−39.92	−26.74	−44.23
	310		−26.21	

The binding constant (K_b) and number of binding site (n) can be determined employing the Scatchard equation, which is given by

$$\log \frac{(F_0 - F)}{F} = \log K_b + n \log[Q]$$

The K_b and n can be calculated by the intercept and the slope of the double logarithm regression curve of log $(F_0 - F)/F$ versus log$[Q]$. According to the values of binding constant (K_b) as shown in Table 4, the platinum complex interacts with HSA and BSA moderately with values of around 10^4–10^5 M^{-1}. In both cases, the value of n is nearly 1, which indicates that there is just one binding site per platinum complex. Comparing the results obtained for the complex studied here with the free ligand, N-benzoyl-N′,N′-dibenzylthiourea ($K_b = \sim 10^3$ M^{-1}) (Correa et al., 2015), it is observed that the coordination of Pt contributes to the increase the albumin affinity.

The combination between compound and protein, such as HSA and BSA, may occur via different types of molecular interactions, including hydrogen bonds, van der Waals, and electrostatic and hydrophobic interactions. The thermodynamic parameters such as ΔG (free energy change), ΔH (enthalpy change), and ΔS (entropy change) are important to evaluate the molecular interactions involved. The thermodynamic parameters shown in Table 4 were calculated from the following equations:

$$\ln \frac{K_{b2}}{K_{b1}} = \left[\frac{1}{T_1} - \frac{1}{T_2}\right] \frac{\Delta H°}{R}$$

$$\Delta G° = -RT \ln K_b = \Delta H° - T\Delta S°$$

where K_{b1} and K_{b2} are the binding constants at temperatures T_1 and T_2, respectively, R is the gas constant, $\Delta G°$ is change in Gibbs free energy, $\Delta H°$ enthalpy changes, $\Delta S°$ entropy changes, and K_b is the equilibrium constant (Ganeshpandian et al., 2014).

The thermodynamic parameters were used to evaluate the intermolecular forces involving the molecules of complex and HSA or BSA. As discussed in the Hirshfeld analysis the complex presents weak interactions to stabilize the crystal packing. These interactions kept the complex-albumin attached, and the characteristic of these interactions can be assigned by the thermodynamic parameters. The values for $\Delta H° > 0$ and $\Delta S° > 0$ imply the involvement of hydrophobic forces in protein binding, $\Delta H° < 0$ and $\Delta S° < 0$ correspond to van der Waals and hydrogen bonding interactions and $\Delta H° < 0$ and $\Delta S° > 0$, suggest an electrostatic force (Ross and Subramanian, 1981).

As observed in Table 5, for HSA the positive $\Delta S°$ and negative $\Delta H°$ values indicate electrostatic forces. On the other hand, for BSA the negative values for $\Delta H°$ and $\Delta S°$ indicate the involvement of van der Waals forces and hydrogen bonding interactions. For both proteins evaluated, the negative values for $\Delta G°$ indicate spontaneous interaction.

4. Conclusion

In the present paper, cis-bis(N-(dibenzylcarbamothioyl)benzamido)platinum(II) complex was synthesized and its molecular structure was correctly determined. When compared with the values for diphenyl and diethyl homologous complexes with square planar geometry, dihedral angle between the chelate planes varied as in the corresponding nickel complexes. Also, the values of intramolecular π–π interaction are very similar to those for the isostructural homologous nickel(II) complex. Hirshfeld surface analysis revealed specific intermolecular contacts such as the crystal determination, and allowed the quantification of their contributions to crystal stabilization. The complex interacts with both HSA and BSA spontaneously, presenting a static mechanism of protein binding modes.

References

Aly, A.A., Ahmed, E.K., El-Mokadem, K.M., Hegazy, M.E.-A.F., 2007. Update survey on aroyl substituted thioureas and their applications. J. Sulfur. Chem. 28, 73–93.

An, X., Zhao, J., Cui, F., Qu, G., 2017. The investigation of interaction between Thioguanine and human serum albumin by fluorescence and modeling. Arab. J. Chem. 10, S1781–S1787. http://dx.doi.org/10.1016/j.arabjc.2013.06.031.

Arslan, H., Flörke, U., Külcü, N., Emen, M.F., 2006. Crystal structure and thermal behaviour of copper(II) and zinc(II) complexes with N-pyrrolidine-N′-(2-chloro-benzoyl)thiourea. J. Coord. Chem. 59, 223–228.

Binzet, G., Flörke, U., Külcü, N., Arslan, H., 2012a. Crystal and molecular structure of bis(4-bromo-N-(diethylcarbamothioyl)benzamido)nickel(II) complex. Eur. J. Chem. 3, 37–39.

Binzet, G., Flörke, U., Külcü, N., Arslan, H., 2012b. Crystal and molecular structure of bis(4-bromo-N-(di-n-butylcarbamothioyl)benzamido)copper(II) complex. Eur. J. Chem. 3, 211–213.

Bourne, S., Koch, K.R., 1993. Intramolecular hydrogen-bond controlled unidentate co-ordination of potentially chelating N-Acyl-N′-alkyl-thioureas: crystal structure of cis-bis(N-benzoyl-N′-propylthiourea)dichloro. J. Chem. Soc. Dalton Trans., 2071–2072.

Correa, R.S., de Oliveira, K.M., Delolo, F.G., Alvarez, A., Mocelo, R., Plutin, A.M., Cominetti, M.R., Castellano, E.E., Batista, A.A., 2015. Ru(II)-based complexes with N-(acyl)-N′,N′-(disubstituted) thiourea ligands: synthesis, characterization, BSA- and DNA-binding studies of new cytotoxic agents against lung and prostate tumour cells. J. Inor. Biochem. 150, 63–71.

Correa, R.S., dos Santos, M.H., Nagem, T.J., Ellena, J., 2012. Host–guest interactions between xanthones and water: the role of O–H⋯O, C–H⋯O, and π⋯π contacts in the channel- and cage-type frameworks. Struct. Chem. 23, 1809–1818.

Correa, R.S., dos Santos, M.H., Nagem, T., Ellena, J., 2010. On the relationships between molecular conformations and intermolecular contacts toward crystal self-assembly of mono, di-, tri-, and tetra-oxygenated xanthone derivatives. Struct. Chem. 21, 555–563.

Cîrcu, V., Ilie, M., Iliş, M., Dumitraşcu, F., Neagoe, I., Păsculescu, S., 2009. Luminescent cyclometallated platinum(II) complexes with N-benzoyl thiourea derivatives as ancillary ligands. Polyhedron 28, 3739–3746.

Das, M., Nasani, R., Saha, M., Mobin, S.M., Mukhopadhyay, S., 2015. Nickel(II) complexes with a flexible piperazinil moiety: studies on DNA and protein binding and catecholase like properties. Dalton Trans. 44, 2299–2310.

Farrugia, L.J., 2012. WinGX and ORTEP for Windows: na update. J. Appl. Crystallogr. 45, 849–854.

Farrugia, L.J., 1997. ORTEP-3 for Windows – a version of ORTEP-III with a graphical user interface (GUI). J. Appl. Crystallogr. 30, 565.

Frizzo, C.P., Martins, M.A.P., 2012. Aromaticity in heterocycles: new HOMA index parametrization. Struct. Chem. 23, 375–380.

Ganeshpandian, M., Loganathan, R., Suresh, E., Riyasdeen, A., Akbarshad, M.A., Palaniandavar, M., 2014. New ruthenium(II) arene complexes of anthracenylappended diazacycloalkanes: effect of ligand intercalation and hydrophobicity on DNA and protein binding and cleavage and cytotoxicity. Dalton Trans. 43, 1203–1219.

Gunasekaran, N., Karvembu, R., Ng, S.W., Tiekink, E.R.T., 2010. 3-Benzoyl-1,1-dibenzylthiourea. Acta Crystallogr. E 66, o2572–o2573.

Hernández, W., Spodine, E., Muñoz, J.C., Beyer, L., Schröder, U., Ferreira, J., Pavani, M., 2003a. Synthesis, characterization and antitumor activity of cis-bis(acylthioureato)platinum(II) complexes, cis-PtL2[HL1 = N,N-diphenyl-N′-benzoylthiourea or HL2 = N,N-diphenyl-N′-(p-nitrobenzoyl)thiourea. Bioinorg. Chem. Appl. 1, 271–284.

Hernández, W., Spodine, E., Richter, R., Hallmeier, K.-H., Schröder, U., Beyer, L., 2003b. Platinum(II) mixed ligand complexes with thiourea derivatives, dimethyl sulphoxide and chloride: syntheses, molecular structures, and ESCA data. Z. Anorg. Allg. Chem. 629, 2559–2565.

Hunter, C.A., 1994. Meldola lecture. The role of aromatic interactions in molecular recognition. Chem. Soc. Rev. 23, 101–109.

Koch, K.R., Bourne, S., 1998. Protonation mediated interchange between mono- and bidentate coordination of N-benzoyl-N′,N′-dialkylthioureas: crystal structure of trans-bis(N-benzoyl-N′,N′-di (n-butyl)thiourea-S)-diiodoplatinum(II). J. Mol. Struct. 441, 11–16.

Knuuttila, P., Knuuttila, H., Hennig, H., Beyer, L., 1980. The crystal and molecular structure of bis(1,1-diethyl-3-benzoyl-thioureato) nickel(II). Acta Chem. Scand. A 36, 541–545.

Macrae, C.F., Edgington, P.R., McCabe, P., Pidcock, E., Shields, G.P., Taylor, R., Towler, M., van de Streek, J., 2006. Mercury: visualization and analysis of crystal structures. J. Appl. Crystallogr. 39, 453–457.

Mihai, S., Negoiu, M., 2012. Synthesis characterization and antitumor activity of platinum(II), palladium(II), gold(III), silver(I), copper (II), rhodium(III) and ruthenium(III) complexes with N-antipirine-N′-benzoylthioureea. Rev. Chim. (Bucharest) 63, 697–702.

Nagasawa, H., Mitsunobu, O., 1981. Alkylation of thioureas and related compounds by use of alcohols, diethyl azodicarboxylate, and triphenylphosphine. Bull. Chem. Soc. Jpn. 54, 2223–2224.

O'Reilly, B., Plutín, A.M., Pérez, H., Calderón, O., Ramos, R., Martínez, R., Toscano, R.A., Duque, J., Rodríguez-Solla, H., Suárez, M., Martín, N., 2012. Synthesis and structural characterization of cobalt(II) and copper(II) complexes with N,N-disubstituted-N′-acylthioureas. Polyhedron 36, 133–140.

Pérez, H., Corrêa, R.S., Duque, J., Plutín, A.M., O'Reilly, B., 2008. cis-Bis(N-benzoyl-N′,N′-dibenzylthioureato-κ²O, S)nickel(II). Acta Crystallogr. E 64, m916.

Pérez, H., Corrêa, R.S., O'Reilly, B., Plutín, A.M., da Silva, C.C.P., Mascarenhas, Y.P., 2012a. Spectroscopic characterization and crystal structure of cis-Bis(N-(2-benzoyl)-N′,N′-diphenylthioureato-k²O, S)nickel(II). J. Struct. Chem. 53, 921–926.

Pérez, H., da Silva, C.C.P., Plutín, A.M., de Simone, C.A., Ellena, J., 2011a. Acta Crystallogr. E 67, m504.

Pérez, H., da Silva, C.C.P., Plutín, A.M., de Simone, C.A., Ellena, J., 2011b. cis-Bis[1,1-dibenzyl-3-(furan-2-ylcarbonyl)thioureato-κ²O, S]copper(II). Acta Crystallogr. E 67, m621.

Pérez, H., O'Reilly, B., Plutín, A.M., Martínez, R., Durán, R., Collado, I.G., Mascarenhas, Y.P., 2011c. Synthesis, characterization, and crystal structure of Ni(II) and Cu(II) complexes with N-furoyl-N′,N′-diethylthiourea: antifungal activity. J. Coord. Chem. 64, 2890–2898.

Pérez, H., Corrêa, R.S., Plutín, A.M., O'Reilly, B., Andrade, M.B., 2012b. Probing the relationships between molecular conformation and intermolecular contacts in N,N-dibenzyl-N′-(furan-2-carbonyl) thiourea. Acta Crystallogr. C 68, o19–o22.

Plutín, A.M., Mocelo, R., Álvarez, A., Ramos, R., Castellano, E.E., Cominetti, R.M., Graminha, A.E., Ferreira, A.G., Batista, A.A., 2014. On the cytotoxic activity of Pd(II) complexes of N,N-disubstituted-N′-acyl thioureas. J. Inorg. Biochem. 134, 76–82.

Rodger, A., Patel, K.K., Sanders, K.J., Datt, M., Sacht, C., Hannon, M.J., 2002. Anti-tumour platinum acylthiourea complexes and their interactions with DNA. J. Chem. Soc. Dalton Trans., 3656–3663

Ross, P.D., Subramanian, S., 1981. Thermodynamics of protein association reactions: forces contributing to stability. Biochemistry 20, 3096–3102.

Sacht, C., Datt, M.S., Otto, S., Roodt, A., 2000a. Synthesis and characterisation of chiral and achiral platinum(II) complexes for potential use as chemotherapeutic agents: crystal and molecular structures of cis-[Pt(L1)2] and [Pt(L1)Cl(MPSO)]; (HL1 = (N,N-diethyl-N′-benzoylthiourea). J. Chem. Soc. Dalton Trans. 5, 727–733.

Sacht, C., Datt, M.S., Otto, S., Roodt, A., 2000b. Synthesis, characterisation and coordination chemistry of novel chiral N,N-dialkyl-N′-menthyloxycarbonylthioureas. Crystal and molecular structures of N,N-diethyl-N′-()-(3R)-menthyloxycarbonylthiourea and cis-(S, S)-[Pt(L)Cl(DMSO)] [where HL = N-(+)- (3R)-menthyloxycarbonyl-N′-morpholinothiourea or N- benzoyl-N′, N′-diethylthiourea]. J. Chem. Soc. Dalton Trans., 4579–4586

Saeed, A., Flörke, U., Erben, M.F., 2013. A review on the chemistry, coordination, structure and biological properties of 1-(acyl/aroyl)-3-(substituted) thioureas. J. Sulfur. Chem. 35, 318–355.

Saeed, A., Florke, U., Erben, M.F., 2014a. The role of substituents in the molecular and crystal structure of 1-(adamantine-1-carbonyl)-3-(mono)- and 3,3-(di) substituted thioureas. J. Mol. Struct. 1065–1066, 150–159.

Saeed, A., Khurshid, A., Jasinski, J.P., Pozzi, C.G., Fantoni, A.C., Erben, M.F., 2014b. Competing intramolecular N–H⋯O=C hydrogen bonds and extended intermolecular network in 1-(4-chlorobenzoyl)-3-(2-methyl-4-oxopentan-2-yl) thiourea analyzed by experimental and theoretical methods. Chem. Phys. 431–432, 39–46.

Sharma, A.S., Anandakumar, S., Ilanchelian, M., 2014. In vitro investigation of domain specific interactions of phenothiazine dye with serum proteins by spectroscopic and molecular docking approaches. RSC Adv. 4, 36267–36281.

Sheldrick, G.M., 2008. A short history of SHELX. Acta Crystallogr. A 64, 112–122.

Spackman, M.A., Jayatilaka, D., 2009. Hirshfeld surface analysis. CrystEngComm. 11, 19–32.

Spackman, M.A., McKinnon, J.J., 2002. Fingerprinting intermolecular interactions in molecular crystals. CrystEngComm. 4, 378–392.

Westra, A.N., Bourne, S.A., Esterhuysen, C., Koch, K.R., 2005. Reactions of halogens with Pt(II) complexes of N-alkyl- and N,N-dialkyl-N′-benzoylthioureas: oxidative addition and formation of an I2 inclusion compound. J. Chem. Soc., Dalton. Trans., 2162–2172

Westra, A.N., Esterhuysen, C., Koch, K.R., 2004. Intramolecular hydrogen-bond-directed coordination: *trans*-bis-(*N*-benzoyl-*N*′-propylthiourea-κS)-diiodoplatinum(II) and *trans*-bis-(*N*-benzoyl-*N*′-propylthiourea-κS)-dibromoplatinum(II). Acta. Crystallogr. C 60, m395–m398.

Wolff, S.K., Grimwood, D.J., McKinnon, J.J., Turner, M.J., Jayatilaka, D., Spackman, M.A. 2009. University of Western Australia.